Evaluating the Feasibility of Electrical Impedance Tomography for Monitoring Knee Angle and Muscle Strength: Towards Application in Total Knee Replacement Rehabilitation

Lishan Liang[1], Tianyang Yao[1], Rokhsaneh Tehrany[2,3], Darren Player[2], Tom Carlson[2], Andreas Demosthenous[1] and Yu Wu[1]

[1]Department of Electronic and Electrical Engineering, University College London, Torrington Place, London WC1E 7JE, UK

[2]Division of Surgery and Interventional Sciences, University College London, Gower Steet, London WC1E 6BT, UK

[3]Therapies, Royal National Orthopaedic Hospital, Stanmore, HA7 4LP, UK

e-mail:lishan.liang.23@ucl.ac.uk, yu.wu.09@ucl.ac.uk

***Abstract*— Rehabilitation following total knee replacement (TKR) principally aims to reduce pain and restore knee muscle strength and function, which necessitates objective monitoring. Given the growing interest in wearable technologies for rehabilitation, this paper investigates the feasibility of using electrical impedance tomography (EIT) to monitor and estimate muscle activity, specifically focusing on resultant knee angle (KA) and muscle strength (MS). A data collection system was designed to simultaneously capture EIT data, kinematic and physiological reference data, namely KA and MS, followed by two experiments. Data processing methods, such as region of interest (ROI) selection and modelling of the correlation between EIT and reference data, were used to assess feasibility. The results indicate that the long short-term memory (LSTM) model achieved an R^2 value of 0.97, suggesting a strong correlation between the EIT data and KA. While EIT demonstrated potential in detecting KA, it did not show effectiveness in capturing changes in muscle activity and MS during isometric contractions.**

Keywords—Electrical impedance tomography, knee Angle and muscle strength monitoring, total knee replacement.

I. INTRODUCTION

Total knee replacement (TKR) surgery involves replacing an osteoarthritic knee joint with an artificial implant aimed at relieving pain and improving mobility. Annually, approximately 700,000 patients undergo TKR surgery in the United States [1], with comparable surgical rates observed in numerous European countries, ranging from 120 to 200 surgeries per 100,000 people [2]. Despite the high success rate of TKR surgery, common post-surgical complications and long recovery periods are inevitably associated. The thigh muscles, such as the quadriceps and hamstrings, exhibit significant strength deficits post-surgery, often requiring extensive rehabilitation to recover fully [3]. In clinical practice, assessing functional recovery is crucial for monitoring progress and tailoring conservative interventions, which commonly aim to restore activities of daily living (ADLs) and physical activity. Isokinetic dynamometers are typically used for recovery practice and quantitative assessment [4], and inertial measurement units (IMUs) [5] are employed in research to measure muscle strength (MS), range of motion (ROM), and knee angle (KA). However, these tools often fail to balance portability and accuracy in home settings [6]. Wearable solutions are beneficial for improving the ability to monitor post-operative recovery.

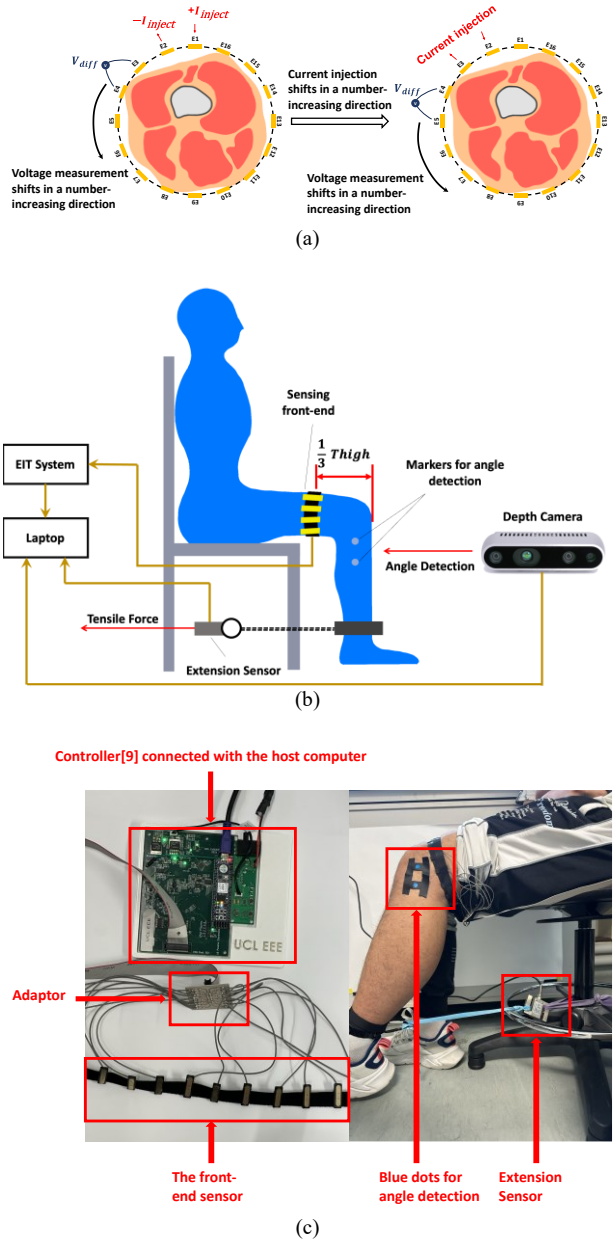

Fig. 1. (a) Sequence of EIT measurements; (b) Overall architecture of the data collection system; (c) Setup showing a user wearing the EIT system.

Electrical impedance tomography (EIT) is a technology used to reconstruct the impedance distribution within the human body. Its wearability and high temporal resolution have demonstrated value in various applications, including non-

invasive monitoring of lung function, cardiac monitoring, and more recently, as potential solutions for monitoring leg motion, as preliminarily illustrated in [7], [8]

Yet, quantitative studies on the correlation between KA and MS in lower limb movements using EIT have not been reported. This study aims to investigate whether EIT can effectively establish a strong correlation with KA and MS using a custom-designed data collection system. The system consists of an EIT system, a vision-based KA capture mechanism, and an MS capture mechanism and is applied in experiments with human participants.

The rest of the paper is organised as follows. Section II describes the design of the data collection system, including both its hardware and software. Section III describes the experiment design and setup for KA and MS measurements, along with the data processing mechanism. Section IV includes data analysis and a discussion of the experimental results. Concluding remarks are presented in Section V.

II. Data Collection System Design

The data collection system is built based on a high-performance EIT system controller [9], which is managed by a field programmable gate array (FPGA). Integrated with the functions of control, waveform generation, digital demodulation, and UART communications, the system is used to capture data from the leg's muscle activities. The EIT operation mainly consists of the current injection and voltage recording executed in a fixed sequence, as shown in Fig. 1(a). A complete rotational measurement corresponds to an EIT frame, which consists of 16 distinct positions for the current injection, and at each current position, 16 voltage measurements are recorded. Each frame consists of 256 measurements. For instance, in the first cycle, current is injected between electrode 1 (E1) and electrode 2 (E2). During this cycle, voltage measurements start at E1 and E2 and then sequentially shift around the electrodes in a number-increasing direction, ending at electrodes E16 and E1. In the second cycle, current injection begins between E2 and E3, with voltage measurements starting at E2 and E3 and continuing through to E1 and E2 after a number-increasing shift. After completing a full frame of 256 measurements, the data undergoes in-phase/quadrature-phase (I/Q) demodulation within the EIT system, and the processed I/Q data is subsequently transferred to the host computer via UART. The Python library – pyEIT [10] was employed to reconstruct the EIT images containing 1024 pixels using the 256 measurements. The EIT image reflects the thigh cross-section in terms of conductivity distribution and is eventually linked to the physical reference data, KA and MS, which are collected simultaneously with the EIT data.

Fig. 1(b) shows the overall system architecture. With the EIT system, the front-end sensors consist of 16 electrodes securely mounted on 3D-printed plastic bases. These electrodes make skin contact for current injection and voltage measurement.

The depth camera shown in Fig. 1(b) is an Intel RealSense D435i used for leg angle detection. The KA measurement process involves using a colour filter to identify and extract two markers placed on the calf. The angle is calculated between the line connecting these two markers and the perpendicular line based on their 3D coordinates. All operations related to the depth camera are developed based on Pyrealsense2.

A digital force gauge (SBT308) was deployed as the extension force sensor shown in Fig. 1(c). To record the extension force, an extension sensor was attached to a resistance band and used to measure the MS of the thigh.

III. Experimental Validation

Two experiments involving KA and MS, alongside EIT measurements, were designed to assess the feasibility of using EIT for detecting knee movements. Five healthy volunteers for each experiment were recruited (a total of 10 males). Participant characteristics were: (1) subjects were healthy adults not previously diagnosed with any disease of the knee and corresponding muscle; (2) were 22 to 25 years old; (3) had a body mass index (BMI) lower than 35 kg/m^2; (4) had provided informed consent [This study was approved by the Ethics Committee of University College London, ID: 27647/004].

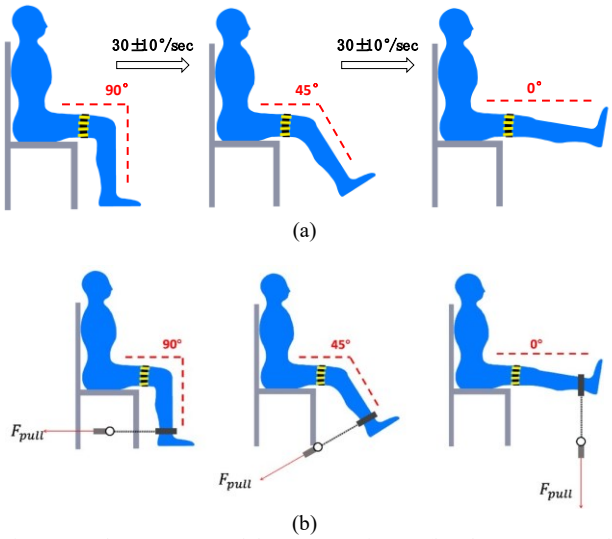

Fig. 2. (a) The movement of the KA experiment. (b) The movement of the MS experiment.

For both experiments, the participants were asked to place the EIT system on their thigh first. A total of 16 electrodes were to be placed evenly on the subject's proximal thigh and one-third of the thigh length from the superior border of the patella. The first electrode was positioned directly opposite the patella. Fig. 1(c) illustrates a diagram of the participant wearing the EIT system. The specific steps of the two experiments are described below. Fig. 2 depicts the movements of the experiments.

(1) KA: These exercises started with the knee joint positioned at a resting angle of 90°, following a starting signal for data acquisition. The knee was then extended to predetermined angles, reaching up to 0° at an angular velocity of 30 ±10 ° /sec, and held at the target angle for 3 seconds. After completing each set of exercises, a stop signal was given to mark the end of the set. Participants were given 5 minutes of rest between each set to prevent fatigue and were instructed to repeat the exercises five times in total.

(2) MS: Muscle strength during isometric contractions was measured as follows. The participant was asked to maintain a sitting position, with the EIT placement requirements identical to the previous experiment. One side of the extension sensor was attached to the ankle, while the other side was connected to the resistance band held by an assistant. After initialising the system, each participant was required to maintain the knee at a specific angle. At the same time, the assistant pulled the resistance band at a steady velocity, with the pulling force registered. Three angle levels, 0°, 45°, and 90°, were applied for the experiment; each angle formed one set of measurements.

Throughout these activities, changes in EIT, along with changes in physical reference data (KA or MS), were simultaneously recorded and tagged with timestamps. Based on these timestamps, the EIT data and reference data were effectively aligned using polynomial interpolation methods.

Essential pre-processing steps were applied to ensure data integrity. To reduce computational load, the collected data was segmented, treating each movement cycle as the smallest unit for analysis. In the KA experiment, one movement cycle began at 90° and ended at 0°, while in the MS experiment, one movement cycle started from a forceless state to a maximum force state.

In addition, to minimise the negative impact of errors, data cleaning was performed at both the dataset level and the unit level. At the dataset level, statistical metrics such as the mean and root mean square (RMS) were calculated for each unit. Units containing obvious outliers were identified and removed. At the individual unit level, the primary concern was the presence of outliers. To address this, polynomial fitting was first employed to estimate the trend of the EIT signal. The estimated trend was then subtracted from the original data to isolate the deviations. Outliers were subsequently detected and removed from the detrended data. The estimated trend was then re-added to the cleaned data. Finally, wavelet transform denoising was applied to remove the high-frequency components, further refining the EIT signal.

To obtain insight into the correlation between KA and MS, the Pearson correlation coefficient (ρ) between the value of each pixel in the EIT images was calculated. Subsequently, pixels with high ρ values are selected as the region of interest (ROI), indicating that changes in EIT image pixel values

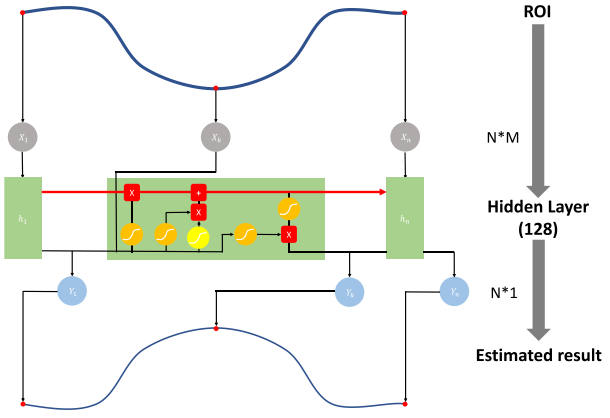

Fig. 3. The structure of the LSTM model. The upper wave represents the averaged pixel value of ROI, while the lower wave indicates the estimated result either KA or MS.

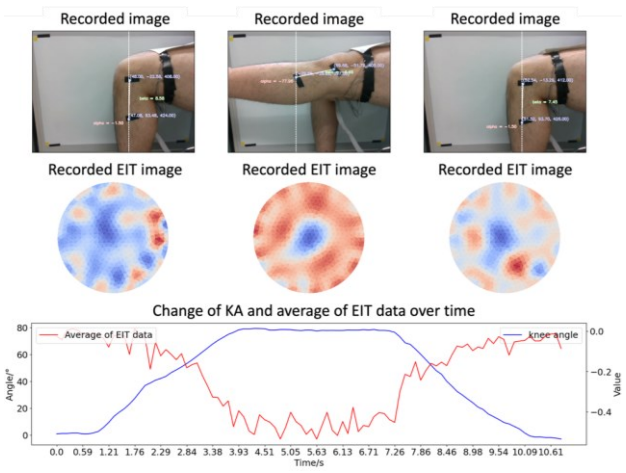

Fig. 4. An example of the collected data in the knee angle experiment. First row displays image frames captured by the depth camera. Second row shows EIT images corresponding to different knee angles. Third row demonstrates the temporal changes in angles and the average EIT data over time.

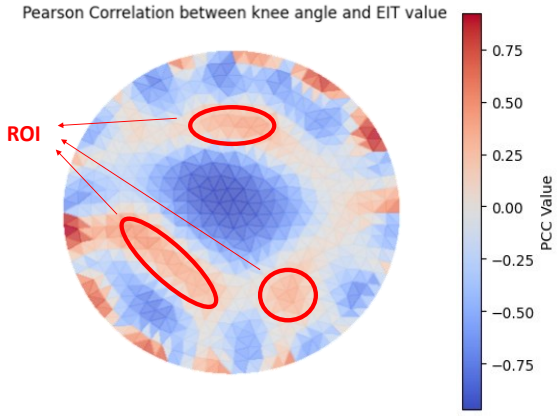

Fig. 5. The ROI selected to reflect the correlation between KA and EIT image pixels.

within these regions are strongly correlated with variations in the physical reference data, namely KA and MS. After the ROI selection, the dimensionality of the EIT data was reduced from $N_i \times 1024$ to $N_i \times M$ ($M << 1024$), where N_i indicates the length of the i unit, M represents the number of features after dimensionality reduction, significantly decreasing the computational load for subsequent model fitting. Given the long-time sequence of the input data, simpler models such as the multilayer perceptron (MLP) and recurrent neural network (RNN) may struggle to capture long-term dependencies between EIT and physical reference data. A long short-term memory (LSTM) network with a single hidden layer comprising 128 neurons was employed for analysis, offering balanced accuracy, and computational efficiency. The structure of the designed model is shown in Fig. 3. To address the issue of unequal time series lengths, a masking technique using the maximum length of the units within the dataset was applied to pad the time series, ensuring that all input datasets conform to the same format. Therefore, the input data, after ROI selection, is in the shape of an $N_{max} \times M$ matrix. Following the transformation by the model, the output is reduced to $N_{max} \times 1$. Based on the length

of the mask, the output data is ultimately trimmed to match the original input length, serving as the estimation result.

IV. Results and Analysis

A. Knee Angle (KA) Test Results

A total of 108 units of movement cycle across 5 participants were collected. One of the recorded units is shown in Fig. 4 as an example, which demonstrates a clear correlation between the KA and EIT ROIs data. After the data pre-processing steps mentioned, the ROIs were extracted through ρ calculation, as shown in Fig. 5. A dataset containing 28 characteristic columns was reformatted based on the ROIs and divided into training and test sets with a ratio of 0.8 for model training. Subsequently, the LSTM shown in Fig. 3 was trained to fit the two datasets, and its performance, along with that of a typical MLP and RNN model, is displayed in Fig. 6 for comparison. In this study, the coefficient of determination (R^2) was used as a key performance indicator to evaluate the goodness of fit between the model and the test set. An R^2 value of 1 represents a perfect fit, with values closer to 1 indicating better model performance. In addition, absolute error was used to provide a more direct representation of the model's prediction accuracy. The LSTM model achieved an R^2 value of 0.97 and an absolute error of 3.28° in angle prediction within the test sets, indicating a strong fit and high accuracy in estimating knee angle. Fig.7 showcases the absolute error over time of an example between the true value and the predicted value by the LSTM model. Based on the results, a conclusion could be drawn that EIT is able to detect the change of KA, and LSTM can be used to represent the correlation between EIT and KA.

B. Muscle Strength (MS) Test Results

A total of 120 units across five participants were collected. Unlike the distribution observed in the analysis of KA, the data for EIT exhibits irregularity with the MS changing. As observed in Fig. 8, data collected under three angle levels show no obvious correlation. When periodic loads were applied to the leg, the EIT data did not exhibit shifts related to the reference data, as seen in the KA experiment. Instead, the data remained in a state with significant noise. Additionally, the correlation coefficient ρ between the two was calculated across all pixels in the EIT distribution, which is visualised in Fig. 9. There are no significantly high ρ values observed in the results, showing that the highest ρ value does not exceed 0.2. Accordingly, it is reasonable to conclude that EIT demonstrates weak performance in detecting MS during isometric muscle contractions.

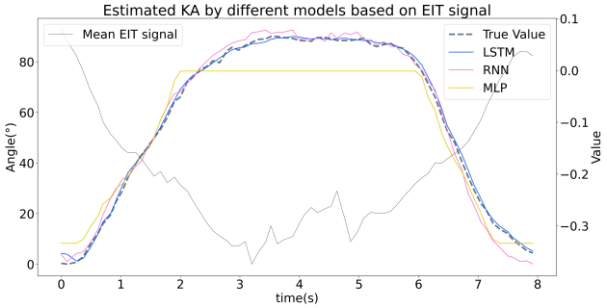

Fig. 6. The performance of the MLP, RNN, and LSTM models was evaluated, with LSTM showing the best fit for modelling KA.

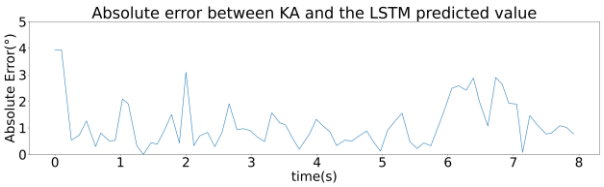

Fig.7. The absolute error between the true value and the predicted value, with the absolute error no more than 4° in this example.

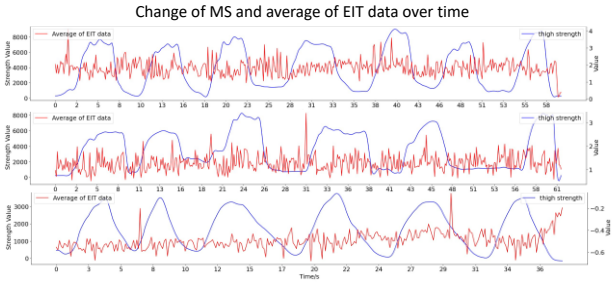

Fig. 8. An example of the data collected during the MS experiment is presented. From top to bottom, the results correspond to knee angles of 0°, 45°, and 90°.

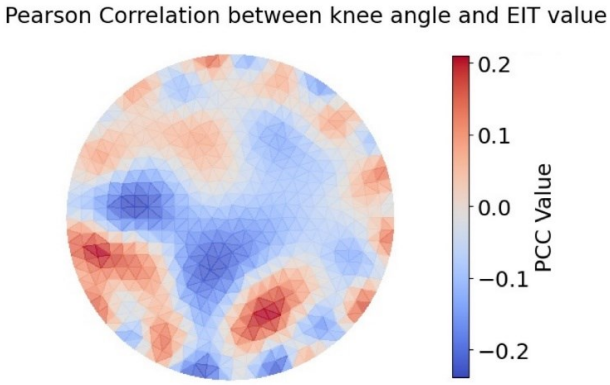

Fig. 9. The distribution of the Pearson correlation coefficient between EIT and MS.

V. Conclusion

In this study, two experiments were designed to evaluate the feasibility of using EIT for detecting KA and MS. The results revealed a strong correlation between EIT measurements and KA, with an R^2 value of 0.97. However, no evidence was found to suggest that EIT effectively captures changes during variations in MS during isometric muscle contractions. Based on these findings and the principles of EIT in monitoring bioimpedance, it is hypothesised that bioimpedance is primarily influenced by the composition of the tested area, including fat, muscle, and bone content. When the muscle is stretched, the composition of the cross-section changes significantly, leading to variations in bioimpedance, which explains the EIT's responsiveness to changes in KA. Conversely, during isometric contractions, the cross-sectional composition remains relatively stable regardless of the applied force, making EIT less sensitive in this context. Therefore, this study demonstrates that EIT is sensitive to significant changes in the cross-sectional area, providing a basis for defining the scope of EIT's applications in future research in TKR.

REFERENCES

[1] I. Fraser, "Facts and Figures 2009. Healthcare Cost and Utilization Project (HCUP)", 2017.

[2] S. M. Kurtz et al., "International survey of primary and revision total knee replacement", Int Orthop, vol. 35, no. 12, pp. 1783–1789, 2011.

[3] Y.-W. Moon, H.-J. Kim, H.-S. Ahn, and D.-H. Lee, "Serial changes of quadriceps and hamstring muscle strength following total knee arthroplasty: a meta-analysis", PloS one, vol. 11, no. 2, p. e0148193, 2016.

[4] M. Li *et al.*, "Better quadriceps and hamstring strength is achieved after total knee arthroplasty with single radius femoral prostheses: a retrospective study based on isokinetic and isometric data", *Arthroplasty*, vol. 2, pp. 1–8, 2020.

[5] A. I. Faisal, S. Majumder, R. Scott, T. Mondal, D. Cowan, and M. J. Deen, "A simple, low-cost multi-sensor-based smart wearable knee monitoring system", *IEEE Sensors J.*, vol. 21, no. 6, pp. 8253–8266, 2020.

[6] D. R. Van der Woude, T. Ruyten, and B. Bartels, "Reliability of muscle strength and muscle power assessments using isokinetic dynamometry in neuromuscular diseases: a systematic review", *Physical Therapy*, vol. 102, no. 10, p. zac099, 2022.

[7] S. Mansouri, Y. Alharbi, F. Haddad, S. Chabcoub, A. Alshrouf, and A. A. Abd-Elghany, "Electrical Impedance tomography--recent applications and developments", *J. Electrical Bioimpedance*, vol. 12, no. 1, pp. 50–62, 2021.

[8] J. Zhu *et al.*, "EIT-kit: An electrical impedance tomography toolkit for health and motion sensing', in *34th Ann. ACM Symp. User Interface Software and Technology*, Virtual Event, USA, 2021, pp. 400–413.

[9] M. Rahal, J. Dai, Y. Wu, A. Bardill, R. Bayford, and A. Demosthenous, "High frame rate electrical impedance tomography system for monitoring of regional lung ventilation", in 2022 44th Ann. Int. Conf. IEEE Eng. Med. Biology Society (EMBC), 2022, pp. 2487–2490.

[10] B. Liu et al., "pyEIT: A python based framework for electrical impedance tomography", SoftwareX, vol. 7, pp. 304–308, 2018.